2006

Fractal Patterns of Coral Communities: Evidence from Remote Sensing (Arabian Gulf, Dubai, U.A.E.)

Samuel J. Purkis
Nova Southeastern University, purkis@nova.edu

Bernhard Riegl
Nova Southeastern University, rieglb@nova.edu

Richard E. Dodge (editor)
Nova Southeastern University, dodge@nova.edu

Return to title

Proceedings of 10th International Coral Reef Symposium, 1753-1762 (2006)

Fractal patterns of coral communities: evidence from remote sensing (Arabian Gulf, Dubai, U.A.E.)

Samuel J. PURKIS*, Bernhard M. RIEGL and Richard E. DODGE

National Coral Reef Institute, Nova Southeastern University Oceanographic Centre, 8000 N. Ocean Drive, Dania FL 33004, USA
*Corresponding author: S. Purkis
FAX: +1-954-262-4098, e-mail: purkis@nova.edu

Abstract In this study, the spatial character of benthic communities is investigated in an Arabian Gulf shallow subtidal carbonate ramp setting, using IKONOS satellite imagery. The patchy distribution of three assemblages of live and dead corals on extensive (but also fragmented) hardground pavements was investigated using a variety of spatial statistics. It was found that the spatial expression of the benthic groups display characteristics that approximate to power-law distributions over several orders of magnitude to an extent that suggests fractal behaviour. Pronounced anisotropy was observed between the spatial patterns in the near-shore and off-shore region which is attributed to different mechanisms of patch formation controlled by the local hydrodynamic regime. The study area is know to be subjected to recurrent and cyclic thermal induced mass mortality events on a decadal time scale, inhibiting reef framework development and likely to be a controlling mechanism in the patchiness of the benthic communities.

Keywords coral, patchiness, spatial anisotropy, scale-invariance, fractal, IKONOS

Introduction

It has long been recognized that the processes driving coral reef dynamics are inherently patchy on many spatial and temporal scales (Mumby and Edwards 2002). Intriguingly, fractal patterns have been observed in the small-scale structure of shallow-water coral colonies (Bradbury and Reichelt 1983; Bassilais 1997) as well as in the frequency distribution of deep-water *Lophelia* corals (O'Reilly et al. 2003; Huvenne et al. 2003). Although fractal analysis of classified satellite imagery has been extensively employed on terrestrial landscapes (De Cola 1994; Burnett and Blaschke 2003) and on tidal flats (Rankey 2002), to our knowledge, this is the first study combining satellite imagery and fractal statistics to quantify the distribution of land cover types beneath the low water mark. The essay builds on the study of Purkis et al. (in press) in the Arabian Gulf and work on the Florida-Bahama platform conducted by Rankey (2002) and Wilkinson et al. (1999), by employing comparable methodology and applying it to sublittoral carbonate facies.

Patches, fragmentation and the landscape

The patch is a key term in spatial analysis. As defined by Rankey (2002), for this study we describe a patch as a discrete, relatively homogeneous spatial domain distinguished by properties unique from surrounding patches. The landscape is defined as a mosaic of distinct patches and represents the study area. For this study the landscape is partitioned into patches through classification of IKONOS satellite data. Clusters of image pixels assigned to a common class are assumed to represent patches of benthos of common character, an assumption validated through statistical accuracy assessment. Patches resolved from image classification are analysed as discrete units in the landscape. In reality, the patch is not an isolated entity, but linked to its neighbours through transport of sediment, nutrients, biota and energy across ephemeral boundaries and connecting corridors. Additionally, classification yields locations of patch boundaries and edge density but not edge strength or width (fuzziness) (Brown et al. 2000) and therefore it is not possible to quantify the strength of the gradient between adjacent facies types and the degree of communication across the boundaries. Despite these pitfalls, satellite imagery provides a synoptic large-scale view of a landscape and is an invaluable tool for quantifying spatial relationships of patches. Lastly, it cannot be overstressed that power-laws are not universal in nature and discipline must be employed when concluding that a natural phenomenon satisfies the fractal condition.

Fractals and the fractal dimension (D)

Fractals have two intrinsic properties, scale-invariance and self- similarity. Scale-invariance means that an object looks the same on all scales and self-similarity, that any part of the system, appropriately enlarged, looks like the whole. In ecology the definition of scale-invariance describes phenomena where scales are ecologically equivalent so that the same ecological conclusions may be drawn from any scale statistically (Li 2000). Fractals generated mathematically are infinite, a

Return to title

property that cannot occur in nature (Halley et al. 2004). Natural fractals are finite and can only be expected to operate as described within certain thresholds. The greater the range of scales over which a fractal pattern persists, the more fractal the system. The literature does not define a critical boundary that must be exceeded before a pattern can be described as fractal. Indeed, Avnir et al. (1998) showed that the majority of cases labelled as fractal in the literature, span only a single decade of magnitude and only rarely achieve 3 decades. Similarly, power-laws identified in the behaviour of lab-scale avalanches typically hold over 1-2 orders (e.g. Jensen 1998). However, Hergarten (2002) postulates that distinguishing a power-law over 2 or fewer decades, requires at least some belief in scale-invariance. In a comparable study, Rankey (2002) identified fractal behaviour in exceedence probability vs. area spanning 3 decades, which we consider to be a reasonable and conservative benchmark and is supported by the literature (Lovejoy 1982; Schroeder 1991).

For earth scientists, the awakening to the relevance of fractal geometry was initiated by the work of Benoit Mandelbrot (1967, 1977). Fractal behaviour is quantified by the fractal dimension (*D*), which can be calculated in many ways, but typically relates to the slope of a power-law relationship. It should be noted that *D* does not provide information on the goodness of fit to a power-function, which in the subsequent analysis is quantified using the adjusted coefficient of determination (R_{adj}^2). R_{adj}^2 values close to 1 indicate a strong relationship and values above 0.90 are considered as a good fit to the power-law (Carlson and Grotzinger 2001). The statistic is used in the following analysis to test the robustness of fractal relationships.

Materials and Methods

Study area

The study site is situated in the south-eastern Arabian Gulf, about halfway between Abu Dhabi and Dubai, near Jebel Ali, in the United Arab Emirates (Fig. 1). For remote-sensing based reef mapping we selected an IKONOS-2 11-bit multi-spectral satellite image acquired on 2nd July 2001 (scene 75209) at 06:49 GMT. The IKONOS imagery was radiometrically calibrated using the coefficients of Peterson (2001) and corrected for the effect of atmospheric path radiance using the empirical line method (Karpoulzi and Malthus 2003). Correction for the water column was conducted according to the protocols presented by Purkis and Pasterkamp (2004) using data pertaining to the apparent optical properties of the water column collected in situ using a suite of inter-calibrated field spectrometers. Bathymetry was extracted from an exhaustive acoustic survey of the area, conducted from a vessel (Riegl and Purkis 2005). The IKONOS satellite imagery was classified using a classifier trained solely by in situ optical measurements of substrate reflectance and yielded a predictive map of sufficient accuracy to identify the spatial distribution of eight facies classes to a depth of six metres (Fig. 1c & Table 1). Accuracy assessment was performed against ground-truthing transects and spot checks (524 validation points) conducted using SCUBA and gave an overall accuracy of 69% and a Tau coefficient of 65%. The level of accuracy is in concert with that of comparable studies using IKONOS in coral-dominated environments (Andréfouet et al. 2003).

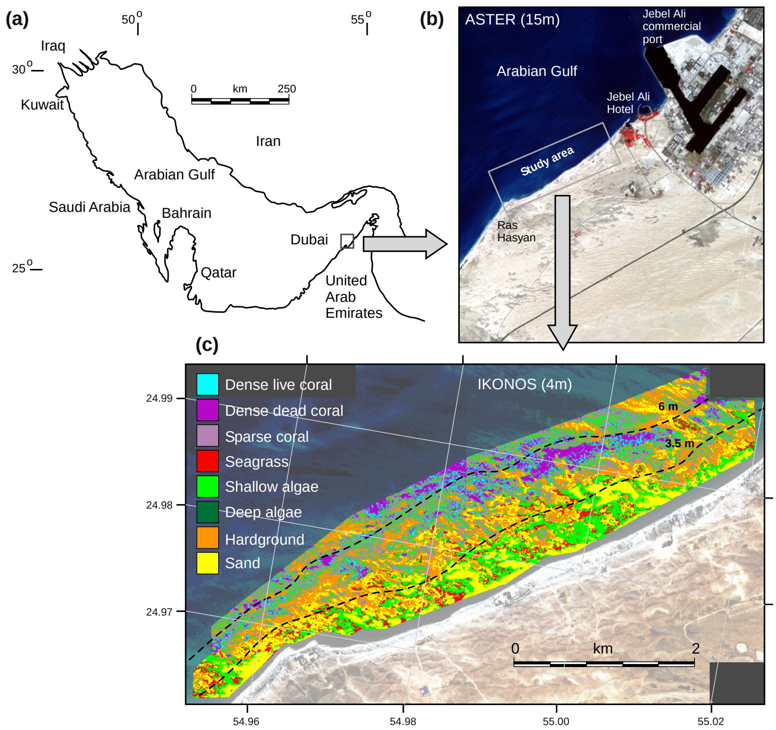

Fig. 1. Location of the study area in relation to the Arabian Gulf (**a**) and highlighted on an ASTER satellite image (spatial resolution 15×15 m) (**b**). The spatial distribution of the submerged facies patterns on the classified IKONOS image (spatial resolution 4×4 m). Isobaths delineate depth in metres (broken black lines) (**c**). Coordinates are decimal latitudes and longitudes.

Table 1. Summary of the typical substrate assemblages encompassed within each of the eight facies classes. Coverage refers to the percentage of the seabed occupied when a 1×1 m area of substrate is viewed from nadir at an altitude of 1 m. Assemblage description is based on Riegl (1999) and Purkis and Riegl (2005).

Facies class	Typical assemblage composition	Comments
Dense live coral	*Porites lutea* and columnar *Porites harrisoni* intermingled with *Favia* spp. & *Platygyra* spp.	Dense colonies over cap-rock, commonly maintaining a low-relief but in places forming non-framebuilding coral carpets. Coverage 50 - 100%
Dense dead coral	*Acropora clathrata* & *A. downingi*	Dense dead tabular colonies, frequently overtopping and heavily overgrown with algal turf and coralline algae. In places the tabular framework has disintegrated into piles of branch rubble. Average size of intact colonies is 1 to 1.5 m and coverage is 80 - 100%
Sparse coral	*Porites, Favia* spp. & *Siderastrea savignyana* with occasional small colonies of *Acropora clathrata*	Widely spaced patches of Faviid and Siderastrea colonies on cap-rock with occasional large *Porites* boulder corals. The *Acropora* were mostly dead at the time of image acquisition. Coverage is generally 10 - 40%
Seagrass	Mainly *Halodule uninervis* with occasional *H. ovalis*	Dense seagrass stands are generally found over sandy-silty substrate and have a coverage of 60 - 80%
Shallow algae	*Rhizoclonium tortuosum*, *Chaetomorpha gracilis* & *Cladophora coelothrix*	Extensive mats over sandy-silty substrates, often associated with seagrasses. Coverage 80 - 100%
Deep algae	*Sargassum binderi*, *S. decurrens*, *Avrainvillea amedelpha* & *Padina* spp.	Moderately dense stands of macro-algae on patches of unconsolidated sediment. Coverage 30 - 60%
Hardground	-	Large slabs of lithified carbonate sediment, fringed by 'tepee' structures. Coverage 100%
Sand	-	Unconsolidated carbonate sand. Coverage 100%

Image analysis

There are a multitude of methods with which to analyse an object for its complexity and fractal character and for this study, we employ a combination of both boundary-based metrics (box-counting) and patch-based metrics (frequency-size distribution and exceedence probability) to investigate the degree to which substrate patches on a submerged shallow carbonate ramp satisfy the fractal condition. Analysis was conducted on the eight-class thematic map of substrate distribution resulting from classification of the IKONOS satellite imagery. The location of patch boundaries were extracted for each of the eight substrate classes by creating a binary image containing only the perimeter pixels of patches of substrate containing a minimum of two connected pixels of constant substrate type. A pixel was considered to be part of the perimeter if it was both nonzero and was connected to at least one zero-valued pixel. Patch area and frequency were computed by extracting the area of all objects within the binary image for each substrate class.

Box-counting

There are numerous permutations of the basic box-counting technique to quantify D, which have been extensively investigated in the literature (Hall and Wood 1993; Pruess 1995; Seuront and Spilmont 2002). In this study, the degree of convolution of the patch boundaries was tested by box-counting according to Rodriguez-Iturbe and Rinaldo (1997) and Turcotte (1997). This technique measures the "wiggliness" of a curve and tests for fractal properties by covering the entire curve with progressively smaller boxes and plotting box size against the number of boxes needed to cover the curve. A straight-line (power-law) relationship in a bilogarithmic plot suggests a fractal and the slope of the resulting function provides an estimate for D (Pruess 1995), the goodness of fit of which can be evaluated using R_{adj}^2.

Frequency-area relations and exceedence probability

Benthic patchiness typically follows a trend where there is a high frequency of small patches in a landscape and large patches are rare. Furthermore the relationship between patch frequency and patch area often approximates to a power-law model (Connell and Keough 1985; Langmead and Sheppard 2004) and has been demonstrated to occur in the study area for all substrate types (Purkis 2004). Exceedence probability for patch area was calculated according to Rodriguez-Iturbe and Rinaldo (1997) and Rankey (2002) under the assumption that a linear relationship between patch area and probability in the log-log domain can be interpreted as further evidence for fractal behaviour. D was taken to be equal to the slope of the resulting power-function plus the Euclidean dimension (here 2, because we consider substrate distribution in plan view and therefore in two-dimensions). The fit was quantified using R_{adj}^2. Power-functions were fitted for each substrate to the portion of the dataset displaying a linear relationship and not for the whole series, since in all cases the data rolled off the trend for smaller patch sizes.

Spatial anisotropy

To test whether geometric patterns are symmetrical across i) the shore-parallel and ii) the shore-perpendicular axes of the studied landscape, patch properties were compared using the previously described metrics. The purpose of investigating symmetry across the shore-parallel axis of the landscape is to ascertain whether the distribution of substrates situated in shallow water have different spatial patterns from those in deeper water. From the three-dimensional description of the study area given by Purkis and Riegl (2005) it is known that the topography of the landscape can be described as a ramp of low-relief (homoclinal) with shore-parallel isobaths. Furthermore, it was recognised that facies zonation in the first 500 m (<3.5 m depth) from shore are characterised by unconsolidated sediments colonised to varying degrees by seagrass and algal mats, which form pronounced shore-parallel elongate structures. Conversely, the zone 1000-1500 m from shore (>4.0 m depth) is characterised mainly by hardgrounds with variable live and dead coral cover and highly fragmented, interspersed with sand and algal patches. Although easily defined by eye, the test investigated whether the spatial metrics are sufficiently sensitive to detect such differences. The landscape was segmented into an inner- and outer-zone using the 3.5 m and 4.0 m isobaths respectively and the full suite of metrics were implemented for sand and algae facies classes, which were common to both zones. To ensure that any difference observed between inner- and outer-zones were not an artefact arising from the partitioning of the dataset, the symmetry of the metrics was also evaluated for all substrate types across the shore-perpendicular axis of the landscape.

Results

Box-counting

Each of the eight substrate types display a robust linear relationship in bilogarithmic plots of box size versus number of filled boxes over nine decades of box reduction (Fig. 2). There is no obvious correlation between substrate type and goodness of fit to the linear slope function, with all data points strictly adhering to the relationship (R_{adj}^2 exceeds 0.99 in all cases) up until the transition towards a horizontal trend beyond 2^{-9}. Image resolution is reached at 2^{11} (equivalent to -12 steps of $\log_2$(box size)) and is the point where the number of boxes equals the number of image pixels. The fact that the log-log relationship rolls off the trend three $\log_2$ cycles prior to reaching the image resolution, suggests that there is a threshold of minimum patch size which must be attained before the definitive spatial trend is satisfied. Counting back from the image resolution (2^{11}) until the point where the linear trend rolls off (2^9), the box size moves from a single image pixel to a box of dimension equivalent to 8×8 pixels. We interpret this to indicate that at least 64 pixels (1024 m^2) are required to properly estimate the size of a patch. The observation is relevant since it suggests that the spatial distribution of patches of lesser area do not display scale-invariance.

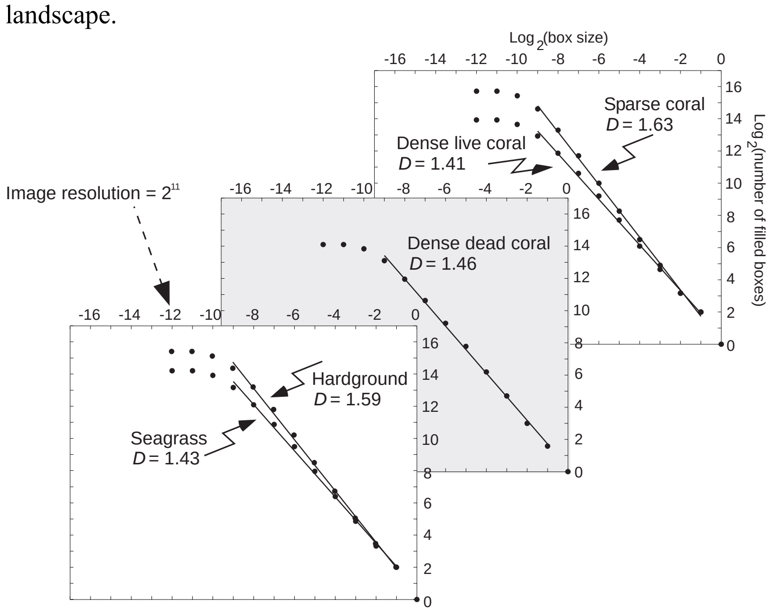

Fig. 2. Implementing the box-counting metric on patch boundaries yields a robust log-log relationship over nine base 2 logarithms of box size. Image resolution is reached at step -12 when box size equals a single image pixel (2^{11}). Box-counted results for sand and algae are given in Fig. 5. In all cases R_{adj}^2 values exceed 0.99, indicating an excellent fit to the power-law (cf. Carlson and Grotzinger 2001).

Frequency-area relations and exceedence probability

The data plotted in Fig. 3 represent the probability (*y* axis) that a given patch will be of an area equal to, or greater than a given area (*x* axis). All substrates are consistent in displaying a decrease in exceedence probability (E.P.) with increasing patch area, confirming the previous observation that the frequency of occurrence decreases when moving from smaller to larger patch sizes (Purkis 2004). Furthermore, all substrates are characterised by a change in the nature of the relationship with an inflection point lying at a patch area of approximately 1000 m^2 (10^3). This is interesting as it corresponds to the observation made during box-counting that patches containing fewer than 64 pixels (1024 m^2) behave differently to larger patches. Furthermore and in concert with the patterns observed with box-counting, it is for patches greater than 1000 m^2 that the probability that the patch size exceeds the area of the *x* axis, rapidly decreases with increasing area and follows a robust power-law. All substrates return $R_{adj}^2 >$ 0.94 which can be described as good power-law relationships (Carlson and Grotzinger 2001) and the data can be inferred to display scale-invariant properties. In order to determine whether the scale-invariance can be

Return to title

interpreted as fractal behaviour, it must be shown to persist over several orders of magnitude. The number of orders spanned is dependent on the slope of the linear regression line and therefore *D*. Facies types spanning the most orders are characterised by higher values of *D* and conspicuously stronger R_{adj}^2 values. Dense live coral and seagrass display scale-invariance over a single order, sparse and dense dead coral extend the range to slightly over 2 orders and hardground as far as 2.5 orders of magnitude (equivalent to patch sizes 1000 m^2 - 500,000 m^2). Although displaying a degree of scale-invariance, it would be misleading to conclude that either seagrass or dense live coral behave as fractals. Similarly the 2 orders offered by dead and sparse corals are not sufficient to characterise explicitly, but according to Avnir et al. (1998) and Jensen (1998), at least suggests fractal behaviour. Hardground is the only facies type to approach 3 orders of scale-invariance and even if the term is used conservatively, would seem a solid candidate for a fractal.

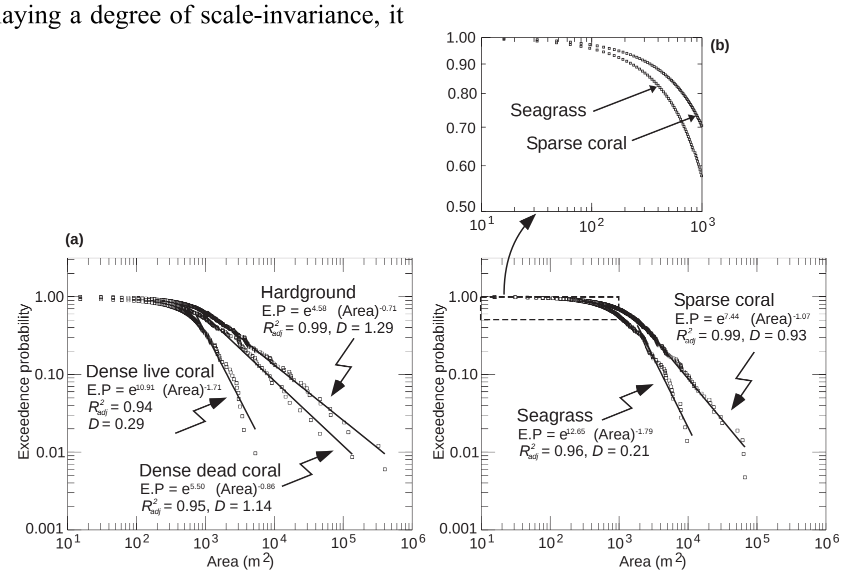

Fig. 3. (**a**) Bilogarithmic plots of exceedence probability (E.P.) vs. area for all facies types (see Fig. 4 for sand and algae). All substrates display a linear trend for patches of area >10^3 m^2, but the slope of the linear function is notably different. Hardground and sparse and dense dead coral display scale-invariance over >2 orders of magnitude, which strongly suggests fractal behaviour. In each case, fractal dimension (*D*) and the power-law equation from which it was calculated, is provided. Goodness of fit to the linear trend is quantified by R_{adj}^2 which exceeds 0.90 in all cases. The inset (**b**) shows the relationship between E.P. and area for sparse coral and seagrass for patch sizes 10^1-10^3 m^2. The expanded E.P. axis demonstrates that the relationship cannot be described by a linear function and therefore it cannot be inferred that the system is bifractal. This is also the case for all other substrates (not shown).

Spatial anisotropy

For both algae and sand, there is a pronounced difference in how the three metrics behave for the inner- and outer-zones (Fig. 4). Box-counting of both substrates reveals that as for previous cases, the relationship rolls off the linear trend beyond box sizes of 2^{-9}, with the inner-zone yielding a lower estimate of *D* than the outer. For the frequency-size distributions of the patches for both sand and algae (Fig. 4b), the pattern is reversed and the inner-zone yields a higher *D*. In both cases the difference in how the metric behaves is systematic, with the power-function of the outer-zone offset above that of the inner. Comparing the relationship between patch area and exceedence probability (Fig. 4c) for sand and algae, yields the most distinct difference in performance of the three metrics. For algae, the outer-zone is inconsistent with all other results by returning a negative *D* (-0.12). The implication being, that the slope of the exponential function is sufficiently abrupt to remain negative following the addition of the Euclidean dimension (2). The abrupt slope only spans a single order of magnitude (10^3-10^4 m^2), which although returning a high R_{adj}^2 (0.98), is not sufficient to be considered fractal. Algae, in the inner zone returns a more typical *D* (1.35) and retains the linear trend over 2.5 orders, which suggests a fractal. Consistent with this pattern, sand returns a higher *D* in the inner- as compared to the outer-zone (1.44 vs. 1.02, respectively), but the R_{adj}^2 of 0.89 for the inner-zone is just below the threshold accepted to indicate a good fit to the power-law (cf. Carlson and Grotzinger 2001). Conversely the outer-zone returns a robust fit (R_{adj}^2 = 0.98) over two orders of magnitude.

Return to title

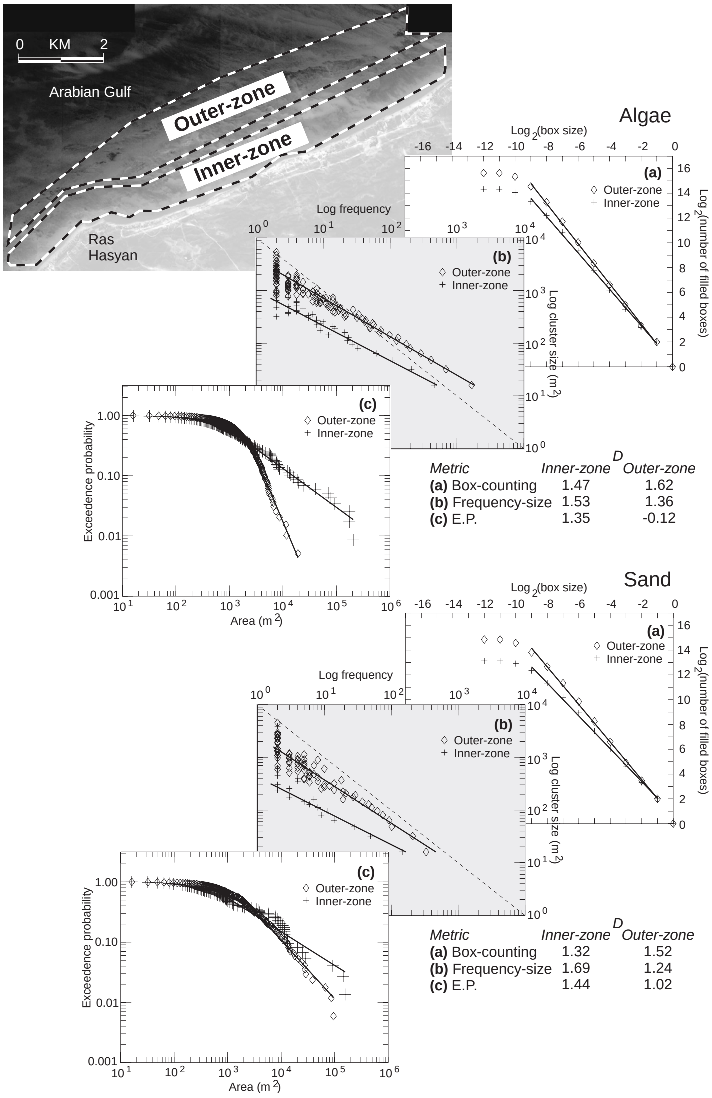

Fig. 4. To test for anisotropy in the spatial distribution of algae and sand, the landscape is partition into an inner- and outer-zone on the basis of the 3.5 m and 4.0 m isobath respectively. For each zone the substrates were investigated using box-counting (**a**), patch frequency-size distributions (**b**) and exceedence probability vs. area (**c**). For the frequency-size plots, patch sizes with an occurrence of <10 have been omitted for clarity. The observed pattern suggests a transition from statistically self-affine (inner-zone) to self-similar (outer-zone) fractal behavior

In summary, it is clear that all three metrics are sensitive to the difference in distribution of sand and algae in water depths less than 3.5 m and greater than 4.0 m. The result is encouraging and indicates that the methodology can differentiate between fairly subtle changes in the spatial expression of substrates. Furthermore, it is seen that the within-metric variation is consistent between substrate types, but there is no consistent trend between metrics. The observation is relevant as it highlights that estimates of *D* behave differently in different metrics, making comparison difficult. The finding supports Lasocki and De Luca (1998), who observe a comparable disparity between metrics through analysis of Monte Carlo generated datasets.

Anisotropy across the shore-perpendicular axis of the study area was tested (Fig. 5) to ensure that the differences between inner and outer-zones did not arise from an artefact related to the partitioning of the dataset. *D* was calculated for each substrate using the three metrics (box-counting, frequency-size and E.P.) and using a t-test for matched pairs was shown not to differ significantly in each case ($P = 0.01$). The result confirms that the anisotropy observed across the 4.0 m isobath is not an artefact. The result also serves to reinforce the hypothesis that the system is truly scale-invariant. The principal of scale-invariance predicts that a spatial distribution will look the same at all scales and so finding that estimates of *D* do not differ significantly when isolated portions of the study area are analysed separately, supports the hypothesis.

Return to title

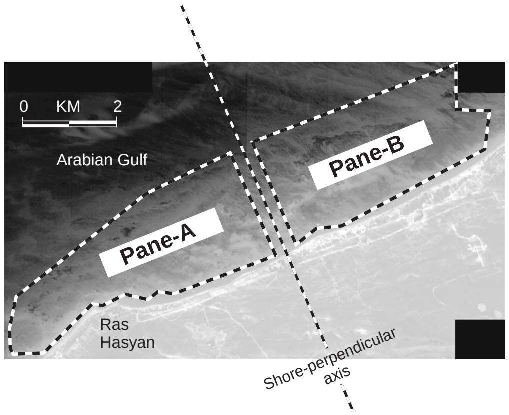

Fig. 5. Comparison of metrics across the shore-perpendicular axis of the landscape to test for anisotropy. For each metric, both D and R_{adj}^2 (not shown) were not significantly different (P = 0.01), supporting the assumption that substrate distribution is scale-invariant.

	Box-counting		**Patch frequency vs. patch size**		**Exceedence probability vs. area**	
Substrate	PANE-A (*D*)	PANE-B (*D*)	PANE-A (*D*)	PANE-B (*D*)	PANE-A (*D*)	PANE-B (*D*)
†Inner-zone algae	1.42	1.44	1.37	1.53	1.37	1.43
Outer-zone algae	1.59	1.59	1.34	1.40	-0.37	0.29
Inner-zone sand	1.25	1.32	1.22	1.11	1.19	1.27
Outer-zone sand	1.46	1.49	1.25	1.25	1.19	0.95
Seagrass	1.40	1.39	1.25	1.28	0.70	0.72
Dense live coral	1.35	1.41	1.23	1.35	0.43	0.59
Dense dead coral	1.35	1.44	1.61	1.59	1.23	1.23
Sparse coral	1.60	1.60	1.22	1.29	1.04	0.85
Hardground	1.55	1.57	1.43	1.49	1.28	1.32

†Inner- and outer-zone refers to the partition of Fig. 4.

Discussion

Analysis of the substrate distribution using a combination of boundary- and patch-based metrics yields evidence of scale-invariance over several orders of magnitude. Most striking is the fact that both a boundary-based (box-counting) and a patch-based (exceedence probability) metric support the observation that 1000 m^2 marks a lower cut-off in size, above which scale-invariance is observed. Whether the failure of the trend at such large patch sizes is an inherent property of both systems, or an edge-effect resulting from the limited size of the landscape, is difficult to judge. With dimensions of 7×1.5 km^2, the study area in Jebel Ali covers an area of approximately 10^7 m^2 and therefore it is not surprising that the linear trend starts to fail. Evidence that the landscape size is a limiting factor would be if the larger patches were seen to be truncated by the landscape boundary, which seems not be the case (Fig. 1c). However, prior to drawing conclusions on the fractal nature of coral reef facies, we would propose re-analysing a larger landscape.

The relevance of spatial anisotropy

Partitioning the landscape into two shore-parallel zones on the basis of the 4 m isobath, demonstrated a pronounced asymmetry in the performance of the fractal metrics for substrates common to both zones (sand and algae). The finding illustrates that a transition zone of self-similar processes occurs around 4 m water depth, for these two substrates. The result is not unexpected as it is known that sedimentation in shallow and therefore high-energy environments, display structures unlike those observed in deeper, more tranquil settings. Of particular relevance to this phenomenon is the action of wave energy dissipating on the shore-line and the depth at which fair-weather wave-base makes contact with the seabed. Personal observation confirms that for the homoclinal ramp of Jebel Ali, the fair-weather wave-base lies at water depths of 3-4 m. At this point, sediment is kept in motion and forms elongate shore-parallel sedimentary features. The Arabian Gulf displays rapid lithification of loose sediment to form early diagenetically cemented hardgrounds (Shinn 1969). It is reasonable to postulate that constant shifting by currents and waves in the nearshore area is necessary to keep sediment unconsolidated, since lithified sediment is absent in water depths <4 m but abundant in deeper areas where the influence of wave action is episodic. The occurrence of hardground provides a suitable substratum for coral recruitment and therefore this is the area where coral assemblages become established. Unconsolidated sand collects in depressions within the coral framework and is colonised to varying extents by algae. The spatial expression of sand and algae in water depths >4 m is one of filling the negative spaces in between patches of coral. Conversely in depths <4 m, sand is not constrained by 'hard' coral patches and forms elongate shore-parallel structures which provide suitable substratum for algal beds. We propose that these two different environments, although both patchy with scale-invariant characteristics, explain the difference observed in the analysis. The disparity in pattern observed between the inner- and outer-zones may also be characterised by a transition from a statistically self-affine to a self-similar fractal pattern. Self-similar fractals are by definition isotropic (e.g. Turcotte 1997) and so the width (x) of a patch should approximately equal its length (y). Indeed, this is likely to be the case in the outer-zone, where patches do not display a pronounced orientation (Fig. 1c) and scale with $x \approx y$. Conversely, for the inner-zone elongate shore-parallel sedimentary features are observed where the patch width (x) is typically greater than the patch length (y). Such a distribution is described as self-affine (Dubuc et al. 1989) and is not isotropic (i.e. $x \neq y$). The observation is in concert with the hypothesis that the fair-weather wave-base is at least partially responsible for the difference in fractal behaviour between zones. With the gradual slope of the Jebel Ali homocline, waves are likely to be orientated parallel to the strike of the shoreline by the time the majority of their energy is dissipated. The inner-zone is the area with maximum topographic gradient, since the slope of the ramp increases abruptly as the shoreline is approached. Here, friction between the seabed and wave-base increases rapidly and wave energy becomes the dominant mechanisms controlling sedimentation.

Fractal patterns and ecological consequences

Having identified patterns that can be defined as fractal in the spatial distribution of facies in Jebel Ali, it is worthwhile postulating which mechanisms may be at work to result in such a fragmented system. The principal factors serving to maintain a patchy landscape are the natural processes of competition for space between adjacent ecological groups (e.g. corals and algae), natural and anthropogenic disturbance and both hydraulically- and bio-mediated erosion. Acting against these, are factors which serve to produce large homogeneous patches of constant facies type. The dominant factors being; sedimentation, growth of a particular biotic group at the expense of a less able competitor and carbonate accretion, through the rapid abiotic lithification of sand sheets (e.g. Shinn 1969) and biotic aragonite production by corals. It is a balance between these two mechanisms that maintains both the universal patchiness and zonation in coral environments. Coral reef landscapes are spatially and temporally non-linear, exhibiting instability at metre to decimetre levels on timescales of months to years, but complex meta-stability at scales of tens of kilometres for decades, centuries and even millennia. In the case of Jebel Ali, the potential for large scale meta-stability as attained by reefs in comparable high-latitude settings (e.g. the Red Sea), is not realised. Based on the size of acroporid colonies and analysis of archive sea surface temperature (SST) data, Purkis and Riegl (2005) confirmed that the area is subjected to recurrent mortality events resulting from cyclic temperature anomalies at a frequency of between 10 and 15 years. Temperature induced mass mortality events in reef environments typically result in a complete killing of corals, followed by a protracted phase-shift to a homogeneous algal dominated environment (Hughes 1994; Bellwood et al. 2004). Conversely, in the Arabian Gulf, compensatory mortality events are observed, disadvantaging the most aggressive coral species (the acroporids) and thus assuring the survival of weaker competitors in the system (e.g. Connell 1978). The relevance being, that the disturbance regime in the Gulf serves to increase heterogeneity and is a plausible candidate for maintaining a highly fragmented landscape with fractal properties. Relating this observation to the fractal dimension (D) of the patch boundaries (as quantified through box-counting), the higher the fragmentation of the landscape, the more complex the patch boundaries become and the higher the value of D is returned. Therefore a high D serves to increase the intimacy of contact between adjacent patches and subsequently promotes 'competition' between adjacent facies groups. Such a situation is likely to maintain spatial instability and prevent (or at least delay) the system from reverting back to a more homogeneous state. Intriguingly, multi-scale randomness (combinations of random processes operating at different resolutions) generate statistical fractal output patterns (Halley 1996, Halley and Kunin 1999). This begs the question whether the fractal patterns observed in the small-scale structure of corals (e.g. Bradbury and Reichelt 1983; Bassilais 1997) are related to the scale-invariance observed at reef-scale? A multi-scale experiment looking at coral structure from colony to reef-scale would be required to shed light on this issue.

Overall relevance and potential applications of fractal patterns

It is commonly recognised that accuracy of image classification in reef environments can be enhanced by combining the spectral content with spatial, structural and textural information, particularly if the target is to identify temporal change (e.g. Andréföuet et al. 2001). Fractal dimension, being an intrinsic property of patch boundaries, offers a potential statistic with which to classify remotely sensed data (e.g. De Cola 1994; Brown et al. 2000). Under the assumption that different facies types have unique patch properties which can be resolved in the imagery, classification can be implemented on the basis of fractal dimension alone (e.g. Myint 2003). Similarly, such an approach could be used in unison with more conventional techniques, but could serve to mitigate many of the problems encountered with the spectral variation of satellite data. Furthermore, fractal dimension is a unique statistic in that it represents a single index summarising the heterogeneity of a landscape. Reef degradation is commonly indicated by a shift to an algal dominated state, accompanied by loss of landscape heterogeneity (Hughes 1994; Bellwood et al. 2004). D is likely to be a useful statistic with which to quantify changes in heterogeneity and has the potential to act as an index of reef status. This is particularly relevant considering the recent advances made in the use of spatial statistical operators on satellite imagery to identify reef degradation through measures of benthic homogeneity as opposed to benthic optical quality (LeDrew et al. 2004).

Acknowledgements

We would like to thank Hiroya Yamano and two anonymous reviewers for helpful comments. BR and SJP were supported by NOAA grant NA16OA1443 to NCRI. The IKONOS image was provided via the NASA Scientific Data Purchase program. This is NCRI contribution 61.

Return to title

References

Andréfouët S, Muller-Karger FE, Hochberg EJ, Hu C, Carder KL (2001) Change detection in shallow coral reef environments using Landsat 7 ETM+ data. Remote Sens Environ 78: 150-162

Andréfouët S, Kramer P, Torres-Pulliza D, Joyce KE, Hochberg EJ, Garza-Perez R, Mumby PJ, Riegl B, Yamano H, White WH, Zubia M, Brock JC, Phinn SR, Naseer A, Hatcher BG, Muller-Karger FE (2003) Multi-sites evaluation of IKONOS data for classification of tropical coral reef environments. Remote Sens Environ 88: 128-143

Avnir D, Biham O, Lidar D, Malcai O (1998) Is the geometry of nature fractal? Science 279: 39-40

Basillais E (1997) Coral surfaces and fractal dimensions: a new method. C R Acad Sc Paris, Life Sci 320: 653-657

Bellwood DR, Hughes TP, Folke C, Nyström M (2004) Confronting the coral reef crisis. Science 429: 827-833

Bradbury RH, Reichelt RE (1983) Fractal dimension of a coral reef at ecological scales. Mar Ecol-Prog Ser 10: 169-171

Brown DG, Jacquez GM, Duh J-D, Maruca S (2000) Accuracy of remotely sensed estimates of landscape change using patch- and boundary-based pattern statistics. In: Huevelink G, et al. (eds) Spatial Accuracy Assessment in Natural Resources and Environmental Sciences. Delft University Press, pp 75-82

Burnett C, Blaschke T (2003) A multi-scale segmentation/object relationship modelling methodology for landscape analysis. Ecol Model 168: 233-249

Carlson J, Grotzinger JP (2001) Submarine fan environment inferred from turbidite thickness distributions. Sedimentology 48: 1331-1351

Connell JH (1978) Diversity in tropical rain forests and coral reefs. Science 199: 1302-1310

Connell JH, Keough MJ (1985) Disturbance and patch dynamics of subtidal marine animals on hard substrata. In: Pickett STA, White PS (eds) The ecology of natural disturbance and patch dynamics. Academic Press, Orlando pp 125-151

De Cola L (1994) Simulating and mapping spatial complexity using multi-scale techniques. Int J Geographical Information Systems 8: 411-427

Dubuc B, Quiniou JF, Roques-Carmes C, Tricot C, Zucker SW (1989) Evaluating the fractal dimension of profiles. Phys Rev A 39: 1500-1512

Hall P, Wood A (1993) On the performance of box-counting estimators of fractal dimension. Biometrika 80: 246-252

Halley JM (1996) Ecology, evolution and 1/f-noise. Trends Ecol Evol 11: 33-37

Halley JM, Hartley S, Kallimanis AS, Kunin WE, Lennon JJ, Sgardelis SP (2004) Uses and abuses of fractal methodology in ecology. Ecol Lett 7: 254-271

Halley JM, Kunin WE (1999) Extinction risk and the 1/f-noise family of noise models. Theor Popul Biol 56: 215-230

Hergarten S (2002) Self-organised criticality in earth systems. Springer, Berlin Heidelberg New York

Hughes TP (1994) Catastrophes, phase-shifts and large-scale degradation of a Caribbean coral reef. Science 265: 1547-1551

Huvenne VAI, De Mol B, Henriet J-P (2003) A 3D seismic study of the morphology and spatial distribution of buried coral banks in the Porcupine Basin, SW of Ireland. Mar Geol 198: 2-25

Jensen HJ (1998) Self-organised criticality. Cambridge University Press, Cambridge

Karpouzli E, Malthus T (2003) The empirical line method for the atmospheric correction of IKONOS imagery. Int J Remote Sens 24: 1143-1150

Langmead O, Sheppard C (2004) Coral reef community dynamics and disturbance: a simulation model. Ecol Model 175: 271-290

Lasocki S, De Luca L (1998) Monte Carlo studies of relations between fractal dimensions in monofractal data sets. Pure Appl Geophys 152: 213-220

LeDrew EF, Holden H, Wulder MA, Derksen C, Newman C (2004) A spatial statistical operator applied to multidate satellite imagery for identification of coral reef stress. Remote Sens Environ 91: 271-279

Li B-L (2000) Fractal geometry applications in description and analysis of patch patterns and patch dynamics. Ecol Model 132: 33-50

Lovejoy S (1982) Area-perimeter relation for rain and cloud areas. Science 216:185-187

Mandelbrot BB (1967) How long is the coast of Britain? Statistical self-similarity and fractional dimension. Science 156:636-638

Mandelbrot BB (1977) The fractal geometry of nature. Freeman, San Francisco

Mumby PJ, Edwards AJ (2002) Mapping marine environments with IKONOS imagery: enhanced spatial resolution can deliver great thematic accuracy. Rem Sens Environ 82: 248-257

Myint SW (2003) Fractal approaches in texture analysis and classification of remotely sensed data: comparisons with spatial autocorrelation techniques and simple descriptive statistics. Int J Remote Sens 24: 1925-1947

O'Reilly BM, Readman PW, Shannon PM, Jacob AWB (2003) A model for the development of a carbonate mound population in the Rockall Trough based on deep-towed sidescan sonar data. Mar Geol 198: 55-66

Return to title

Peterson B (2001) IKONOS relative spectral response and radiometric calibration coefficients. Document number SE-REF-016, Rev. A. Space Imaging, Inc., Thornton, CO.

Pruess SA (1995) Some remarks on the numerical estimation of fractal dimension, In: Barton CC, La Pointe PR (eds) Fractals and the earth sciences. Plenum Press, New York London

Purkis SJ (2004) Calibration of satellite images of reef environments. Ph.D. Thesis, Vrije Universiteit, Amsterdam, 205 pp. ISBN 90-9018043-5

Purkis SJ, Pasterkamp R (2004) Integrating in situ reef-top reflectance spectra with Landsat TM imagery to aid shallow-tropical benthic habitat mapping. Coral Reefs 23: 5-20

Purkis SJ, Riegl B (2005) Spatial and temporal dynamics of Arabian Gulf coral assemblages quantified from remote-sensing and in situ monitoring data. Mar Ecol-Prog Ser 287: 99-113

Purkis SJ, Riegl B, Andréfouët S (in press) Remote sensing of geomorphology and facies patterns on a modern carbonate ramp (Arabian Gulf, Dubai, U.A.E.). J Sediment Res

Rankey EC (2002) Spatial patterns of sediment accumulation on a Holocene carbonate tidal flat, Northwest Andros Island, Bahamas. J Sediment Res 72: 591-601

Riegl B, Purkis SJ (2005) Detection of shallow water corals from IKONOS satellite and QTC View (50, 200 kHz) single-beam sonar data (Arabian Gulf; Dubai; UAE). Remote Sens Environ 95: 96-114

Rodriguez-Iturbe I, Rinaldo A (1997) Fractal river basins: chance and self-organization. Cambridge University Press, Cambridge

Schroeder M (1991) Fractals, chaos, power laws: minutes from an infinite paradise. Freeman, New York

Seuront L, Spilmont N (2002) Self-organised criticality in intertidal microphytobenthos patch patterns. Physica A 313: 513-539

Shinn EA (1969) Submarine lithification of Holocene carbonate sediments in the Persian Gulf. Sedimentology 12: 109-144

Turcotte DL (1997) Fractals in geology and geophysics. Cambridge University Press, Cambridge

Wilkinson BH, Drummond CN, Diedricht NW, Rothman ED (1999) Poisson processes of carbonate accumulation on Paleozoic and Holocene platforms. J Sediment Res 69: 338-350